Ecological Indicators 93 (2018) 24–35

Contents lists available at ScienceDirect

Ecological Indicators

journal homepage: www.elsevier.com/locate/ecolind

Original Articles

The impacts of climate change and human activities on alpine vegetation and permafrost in the Qinghai-Tibet Engineering Corridor

Lihui Luo[a,b,*], Wei Ma[b,*], Yanli Zhuang[c,*], Yaonan Zhang[a], Shuhua Yi[d], Jianwei Xu[e], Yinping Long[f], Di Ma[a], Zhongqiong Zhang[b]

[a] Cold and Arid Regions Environmental and Engineering Research Institute, Chinese Academy of Sciences, Lanzhou, Gansu Province 730000, China
[b] State Key Laboratory of Frozen Soils Engineering, Cold and Arid Regions Environmental and Engineering Research Institute, Chinese Academy of Sciences, Lanzhou, Gansu Province 730000, China
[c] Linze Inland River Basin Research Station, Key Laboratory of Inland River Basin Ecohydrology, Cold and Arid Regions Environmental and Engineering Research Institute, Chinese Academy of Sciences, Lanzhou, Gansu Province 730000, China
[d] State Key Laboratory of Cryospheric Sciences, Cold and Arid Regions Environmental and Engineering Research Institute, Chinese Academy of Sciences, Lanzhou, Gansu Province 730000, China
[e] Hunan University of Arts and Science, Changde, Hunan Province 415000, China
[f] Chengdu University of Information Technology, Chengdu, Sichuan Province 610225, China

ARTICLE INFO

Keywords:
Alpine vegetation
Permafrost
Climate change
Human activities
NDVI
Active layer thickness

ABSTRACT

The Qinghai-Tibet Engineering Corridor (QTEC) in China may reflect the changes in the alpine ecosystem of the Qinghai–Tibet Plateau (QTP) that are driven by global climate change combined with intensive human activities. We used the normalized difference vegetation index (NDVI) as an indicator of alpine vegetation activity and the permafrost active layer thickness (ALT) as an indicator of permafrost dynamics to understand the impacts of climate change, human activity, or their combination on the alpine ecosystem in the QTEC. Based on the types of frozen ground, we separated the QTEC into northern, permafrost, and southern zones. The surface air temperature increased by 0.28 °C per decade from 1982 to 2010, and the rising trend of air temperature was most prominent in the permafrost zone ($P < 0.05$); the total precipitation exhibited a significant increase of 15 mm per decade ($P < 0.05$). The level of human activity in the QTEC rose slowly before 2000 and rapidly after 2000. The NDVI trends over the QTEC increased over the past thirty years, but the NDVI declined in some areas from 2001 to 2010, especially in the southern QTEC. The permafrost in the QTEC continued to thaw, and the ALT increased. Our results indicated that the QTEC experienced a significant warming and wetting trend. The increased precipitation improved the alpine vegetation activity across much of the QTEC, and the increased air temperature accelerated the thawing of permafrost. However, the construction and operation of the Qinghai–Tibet Railway since 2001 and 2006 promoted an influx of residents and tourists, boosted the local economy, and resulted in the deterioration of the alpine vegetation, particularly in the southern QTEC. Moreover, our results suggested that improvement of alpine vegetation cannot necessarily prevent permafrost degradation caused by warming.

1. Introduction

Climate change and human activities can significantly impact the underlying permafrost via vegetation and the active layer (Chen et al., 2014; Guglielmin et al., 2014). Climate-induced warming of the near-surface atmosphere and the corresponding rise in ground temperatures will lead to substantial changes in the water and energy balance in areas underlain by permafrost (Hilbich et al., 2008). Human activities cause additional disturbances, including overgrazing, numerous engineering projects, and the rapid growth of the population. In particular, the construction and operation of engineering infrastructures can change the original ground surface conditions in permafrost regions, causing degradation of the permafrost and the associated ecological environment (Jin et al., 2008).

Vegetation is the medium for heat exchange between the atmosphere and the lithosphere, and, as a result, changes to vegetation and the associated areas can directly impact permafrost (Guglielmin et al., 2014; Royleveillee et al., 2014; Runyan and D'Odorico, 2012; Yi et al., 2014). Vegetation can control soil temperature, the amount of water reaching the permafrost active layer (Runyan and D'Odorico, 2012),

* Corresponding authors at: Cold and Arid Regions Environmental and Engineering Research Institute, Chinese Academy of Sciences, Lanzhou, Gansu Province 730000, China (L. Luo).
E-mail addresses: luolh@lzb.ac.cn (L. Luo), mawei@lzb.ac.cn (W. Ma), zhuangyl@lzb.ac.cn (Y. Zhuang).

https://doi.org/10.1016/j.ecolind.2018.04.067
Received 20 February 2017; Received in revised form 24 April 2018; Accepted 25 April 2018
Available online 30 April 2018
1470-160X/ © 2018 Elsevier Ltd. All rights reserved.

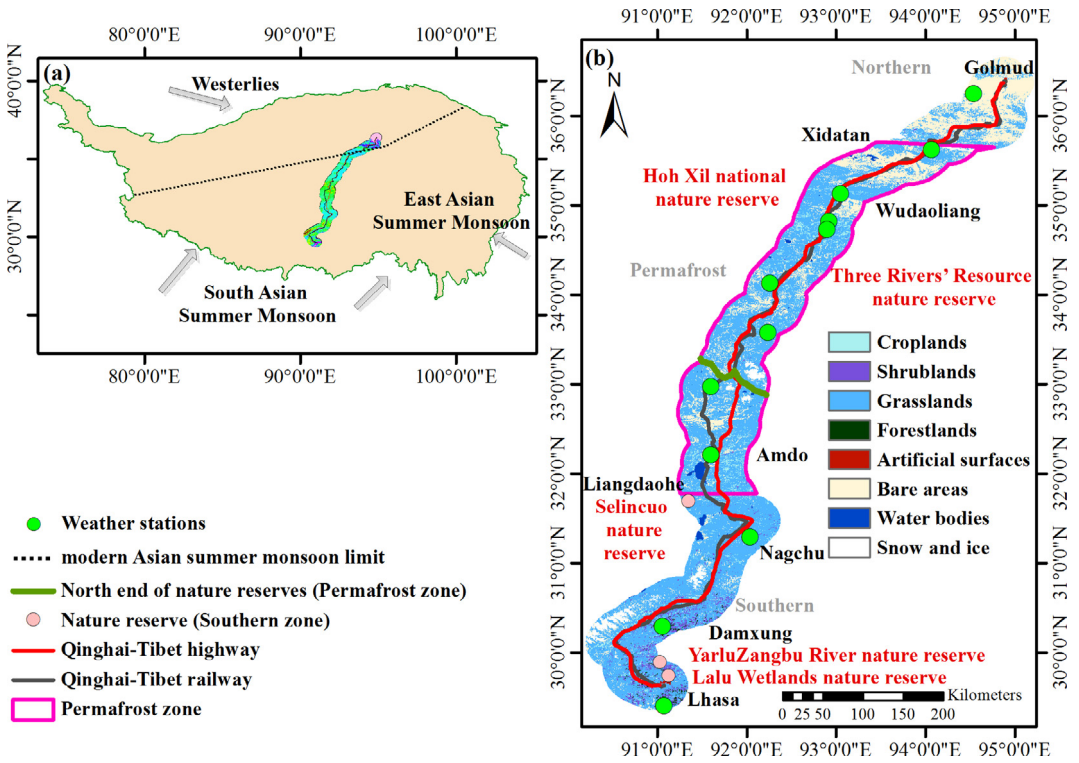

Fig. 1. Geography of the QTEC area. (a) Location of the QTEC (central area). (b) Some of the related weather stations (green points), Qinghai-Tibet Railway (black line), Qinghai-Tibet Highway (red line), permafrost zone (pink box), and the southern end of the nature reserves (green line), and the northern end of the nature reserves (the top of the pink box). (For interpretation of the references to colour in this figure legend, the reader is referred to the web version of this article.)

and snow accumulation (Royleveillee et al., 2014). Vegetation affects the energy balance of the soil; thus, changes in vegetation can provide feedback to the active layer thickness (ALT) and the temperature at the top of the permafrost (Guglielmin et al., 2014). The presence of different vegetation types helps preserve the permafrost layer by maintaining low soil temperatures. Different vegetation types produce different organic layer thicknesses (Royleveillee et al., 2014), and the organic layer of vegetation provides an insulating effect on the ground-surface temperature, which can slow permafrost degradation (Guglielmin et al., 2014; Runyan and D'Odorico, 2012). Permafrost degradation affects the hydrology and biogeochemistry of ecosystems and the engineering infrastructures above the permafrost (Jin et al., 2008). Active layer thickening and permafrost warming result in general decreases in the groundwater content (Guglielmin et al., 2014; Jin et al., 2008; Runyan and D'Odorico, 2012; Yi et al., 2014) and the numbers of families and species of plants (Yang et al., 2013); moreover, these changes profoundly enhance vegetation succession (Jin et al., 2008; Yang et al., 2013).

As the sole and highest physiographic unit of average elevation on Earth, the Qinghai–Tibet Plateau (QTP) is called the "Third Pole" and plays a key role in the Asian summer monsoon (Liu et al., 2012; Wu et al., 2015a). The QTP is of utmost relevance for the atmospheric circulation that is mainly controlled by the mid-latitude westerlies and the Asian summer monsoon (ASM), including the South Asian summer monsoon (SASM) and East Asian summer monsoon (EASM) (Bothe et al., 2011). The linkage of the Iranian Plateau to the QTP substantially increases precipitation over the Arabian Sea and the north Indian subcontinent, effectively contributing to the development of the SASM (Liu et al., 2012). The changes in the thermal forcing, precipitation, and surface pressure over the QTP are closely correlated with the changes in the ASM (Bothe et al., 2011; Liu et al., 2012). The air temperature over the QTP has increased by 0.28 °C per decade over the past 50 years (Li et al., 2010; Shen et al., 2015), and the precipitation has also shown an overall slight increase (Chen et al., 2013). Before 1990, the overall scale of human activities was small, and the impacts of human activities on the ecosystems were also less pronounced. Negative effects of human activities on the environment in the area occurred simultaneously and intensively from 1990 to 2000. After 2000, the scale of human activities increased with the construction of the Qinghai-Tibet Railway (QTR) (Fan et al., 2015). The increases in climate warming and total precipitation and the intensification of human activities across the QTP over the past several decades (Li et al., 2010) have resulted in vegetation improvements in most of the region (Chen et al., 2014; Cuo et al., 2016; Zhang et al., 2013), permafrost warming, and active layer thickening (Cheng and Wu, 2007; Harris, 2010; Jin et al., 2008; Wu et al., 2015b; Wu and Zhang, 2010). However, the vegetation has worsened in some areas (Shen et al., 2015).

The Qinghai–Tibet Engineering Corridor (QTEC) is situated in the central QTP and is classified as a critical engineering and transportation corridor that connects the inland of China and the Tibetan Plateau (Luo et al., 2017). Most previous studies focused on the impacts of climate change on the ecologically important QTP, and little attention has been paid to the much smaller area of the QTEC (Chen et al., 2014; Li et al., 2010; Wu and Zhang, 2010; Zhang et al., 2013). However, the QTEC is a typical indicator of the current climate conditions and human impacts that reflect the ecosystem changes in the QTP because the QTEC is affected by global climate change combined with environmental disturbances from human activities. We divided the study duration into two periods to evaluate the impacts of human activities on the changes in vegetation because human activities increased around 2000, especially with the construction of the QTR. To further understand the impacts of global climate change and human activities on the changes in alpine vegetation and permafrost over the QTEC, we 1) explored the spatiotemporal patterns of vegetation and climate factors in three different frozen soil zones, 2) evaluated the effects of human activities on the changes in vegetation, especially in the last decade when the level of human activities increased, and 3) analyzed the effects of vegetation on permafrost.

2. Data and methods

2.1. Study area

The QTEC is approximately 60 km wide and stretches for approximately 1120 km from Geermu (Golmud) in Qinghai Province to Lhasa in the Tibet Autonomous Region. This naturally occurring north–south corridor in the central area of the QTP includes important engineering infrastructures, such as the QTR and Qinghai-Tibet Highway (QTH), a petroleum pipeline, high-tension line, communication optical fiber cable, and others (Fig. 1). The average elevation in the corridor is approximately 4700 m, with approximately 80% of the area exceeding 4000 m and a 50-km stretch exceeding 5000 m (Jin et al., 2008). Permafrost is an important feature of the QTEC, extending for approximately 531 km from Xidatan (35.62 °N, 94.07 °E) to Liangdaohe (31.82 °N, 91.73 °E). The temperature ranges from a mean monthly minimum of −30 °C in the winter to a mean monthly maximum of 25 °C in the summer. The annual mean precipitation is 50–400 mm, and 80% of which occurs from May to September, with the maximum from July to August (Jin et al., 2008). Quaternary sediments consist of silty clay, loam, clay, and sand. The dominant soil type is *Gelic Leptosols*, which is found in approximately 70% of the area (Nachtergaele et al., 2009). The areas beyond the southern and the northern ends of the permafrost are seasonally frozen. Long-term soil temperature measurements indicate that the lower altitudinal limit of the permafrost has risen 25 m over the last 30 years in the north and between 50 and 80 m over the last 20 years in the south (Cheng and Wu, 2007). For the purposes of this study, the QTEC was divided into three zones: the northern edge of the permafrost (called “the northern zone”), the permafrost, and the southern edge of the permafrost (called “the southern zone”) (Fig. 1). The Hoh xil National Nature Reserve and the Three River Sources Nature Reserve were established in 1997 and 2000 in the northwest and southeast of the QTH, respectively, and both are in permafrost zones. In the southern zone, there are three smaller nature reserves.

2.2. Data

Most of the area of the corridor is a semi-arid, gently rolling, grassland landscape. Vegetation classification data for the study were derived from the global land cover classification product Globcover V2.3 (Bontemps et al., 2011). The vegetation along the QTEC is dominated by alpine steppe and meadow and includes desert, alpine steppe, alpine meadow, marsh, and alpine shrubland. The northern zone is a typical desert; alpine steppes and meadows are distributed in the permafrost zone, and alpine meadow and shrubland are found mainly in the grazing and farming areas in the southern zone.

The normalized difference vegetation index (NDVI) is an indicator of vegetation activity (photosynthesis and vegetation cover) (White et al., 2016). In this study, NDVI was used to characterize vegetation changes using satellite-derived datasets. High-resolution NDVI data for 1982–2010 (available at http://daac.gsfc.nasa.gov/) were derived from the Global Inventory Modeling and Mapping Studies (GIMMS) of Advanced Very High Resolution Radiometer (AVHRR), which is located on a National Oceanic and Atmospheric Administration (NOAA) polar-orbiting satellite; this NDVI product has a spatial resolution of 5 km and a temporal resolution of 15 days (GIMMS 3g.v1 available at https://ecocast.arc.nasa.gov/data/pub/gimms/) (Nemani et al., 2009). The moderate-resolution imaging spectroradiometer (MODIS) NDVI product has a spatial resolution of 250 m and a temporal resolution of 16 days; we used these data from 2001 to 2010 (Chen et al., 2006). NDVI data for the growing season (May–September) were used to infer vegetation growth.

Meteorological data were obtained from the China Meteorological Administration (http://www.cma.gov.cn/) from permanent meteorological stations across the QTP. Fourteen weather stations (of the 99 total in the QTP) were selected near the QTEC, and 3-h-interval meteorological records were collected from 1982 to 2010. The weather station data were spatially interpolated, and then fusion datasets of GLDAS (Rui and Beaudoing, 2011), GEWEX (Coughlan and Avissar, 1996) and TRMM (Huffman et al., 2007) were created to produce a new dataset for 1982–2010 with a spatial resolution of 0.1° and a temporal resolution of 3 h.

Data describing human activity were acquired from China’s third to sixth population censuses (the National Bureau of Statistics of China, http://data.stats.gov.cn) and a 1 km grid population dataset of China (Global Change Research Data Publishing and Repository, http://www.geodoi.ac.cn), and these data included the size and spatial distribution of the population (Fu et al., 2014) and grazing intensity.

2.3. Methods

Formula (1) was used to calculate the long-term trends of variables such as precipitation, air temperature, wind speed, downward radiation, NDVI and ALT.

$$\text{Slope} = \frac{n\times\sum_{i=1}^{n}(i\times \text{factor}_i)-(\sum_{i=1}^{n} i)\times(\sum_{i=1}^{n}\text{factor}_i)}{n*\sum_{i=1}^{n} i^2-(\sum_{i=1}^{n} i)^2} \quad (1)$$

The *factor* in Formula (1) represented these variables, where $factor_i$ is the variable in year *i,* and *n* represents the total number of years. Using NDVI as an example, a positive slope value meant that NDVI was increasing and indicated an improvement in vegetation conditions (such as an increase in cover), while a negative value meant that NDVI was decreasing and indicated a degradation in vegetation conditions; a slope of zero suggested no change (Chen et al., 2014).

The permafrost model predicted the spatio-temporal variation of the thermal response of permafrost to the changing climate conditions and the surface and subsurface properties of the earth (Riseborough et al., 2008). Thawing depths can be computed using accumulated air degree-days, with thawing degree-days of air (Celsius degree-days) > 0 as the climatic index commonly used for comparisons based on a variant of the Stefan solution (Sazonova and Romanovsky, 2003). We simulated the maximum thawing depth (ALT) to quantify the permafrost dynamics using the Stefan solution (Nelson et al., 1997) (Formulas (2) and (3)). The Stefan solution has been widely used for spatial characterization of the active layer in the QTP using summer air temperature records and active-layer data (Riseborough et al., 2008). In this study, the parameters of the Stefan solution were based on soil classification data (Nachtergaele et al., 2009), field observations, and topographic maps. The Stefan solution calculates the ALT by relating it to the thermal conductivity of the ground in a thawed state, dry bulk density, volumetric water content in a thawed state, and volumetric unfrozen water content in a frozen state (the volumetric unfrozen water content was assigned to 5%). There are four types of soil: silty clay, loam, clay, and sand. Dry bulk density and water contents were determined by measurements in the four soil types in the study area. Then, based on the physical and mechanical parameters of frozen soil, the thermal parameters of the soil were determined (Table 1).

Table 1
Symbols used in the equations.

Variable	Meaning	Unit	Value
ALT	Active layer thickness	m	
T_a	Thawing degree-days of air	°C	
T	Air temperature	°C	
λ_t	Thermal conductivity of ground in a thawed state	W/m °C	0.53–1.58
L	Latent heat of fusion	J/kg	$3.35 * 10^5$
γ	Dry bulk density	kg/m^3	900–1800
W	Volumetric water content in a thawed state	%	6–17
W_u	Volumetric unfrozen water content in a frozen state	%	5

$$ALT = \sqrt{\frac{2\lambda_t \times T_a}{L\times\gamma \times (W-W_u)}} \quad (2)$$

$$T_a = \sum_{1}^{n} T, \text{ where } T > 0 \quad (3)$$

We used linear regression analyses and Pearson correlation coefficients to analyze the spatial distributions and changes over the past 30 years of meteorological factors, human activities, NDVI, and the ALT for each zone of the QTEC.

The spatial distribution of the local population was based on Landsat TM data (available at https://lta.cr.usgs.gov/TM). First, the spatial characteristics and regional differences in the population distribution in the corridor were analyzed. Then, the urban population density, traffic conditions, DEM, and total population were determined.

3. Results

3.1. Regional climate change

The surface air temperature increased by 0.28 °C per decade during the period from 1982 to 2010. The total precipitation levels exhibited a significant increase of 15 mm per decade ($P < 0.05$). Downward radiation (including shortwave and longwave), exhibited a slightly upward trend, with a rate of increase of 1.14 W/m^2 per decade. Downward longwave radiation exhibited a rising trend ($P < 0.05$), while downward shortwave radiation exhibited a decreasing trend ($P < 0.05$). The surface wind speed exhibited a decline of −0.32 m/s per decade.

The air temperature was strongly influenced by altitude, with the permafrost zone exhibiting the lowest mean annual air temperature (Fig. 2). The mean annual surface air temperatures in the northern, permafrost, and southern zones increased by 0.02, 0.03, and 0.03 °C yr^{-1}, respectively, during 1982–2010. The southern and permafrost zones exhibited larger changes than the northern zone, and the changes in air temperature in the permafrost zone were similar to the maximum change observed in the southern zone. However, the increase in the annual total precipitation in the permafrost zone was the largest, followed by that in the northern and southern zones. The annual total precipitation in the three zones increased continuously at rates of 1.26, 2.00, and 0.91 mm yr^{-1} from north to south, respectively. The mean annual downward radiation exhibited a slightly upward trend with slopes of 0.08, 0.13, and 0.10 W m^{-2} yr^{-1} from north to south, respectively. The mean annual wind speed declined with slopes of −0.04, −0.04, and −0.02 ms yr^{-1} in the 3 zones from north to south, respectively, with the southern zone exhibiting minimum changes. The four meteorological factors among the zones indicated that the changes were largest in the permafrost zone.

3.2. Human activities

The engineering and transportation corridor is the most frequented and densely populated area in the QTP. Since the QTH was built in 1973, the infrastructure in the QTEC has expanded, and the QTH continues to be renovated and maintained. For example, the Golmud to Lhasa Oil Products Pipeline was constructed in 1972–1977, the Lanzhou–Xining–Lhasa Fiber-Optics Cables were installed in 1997, the 110-kV transmission line was installed in 2005–2006, and the opening of the QTR between 2001 to 2006 increased traffic (Jin et al., 2008). Human activities in the QTEC differed across the three zones. Livestock-raising, construction and operation of engineering infrastructure, and tourism were the main types of human activities in the northern zone and the southern QTEC, including the southern zone and the southern part of the permafrost zone. The nature reserves in the permafrost zone

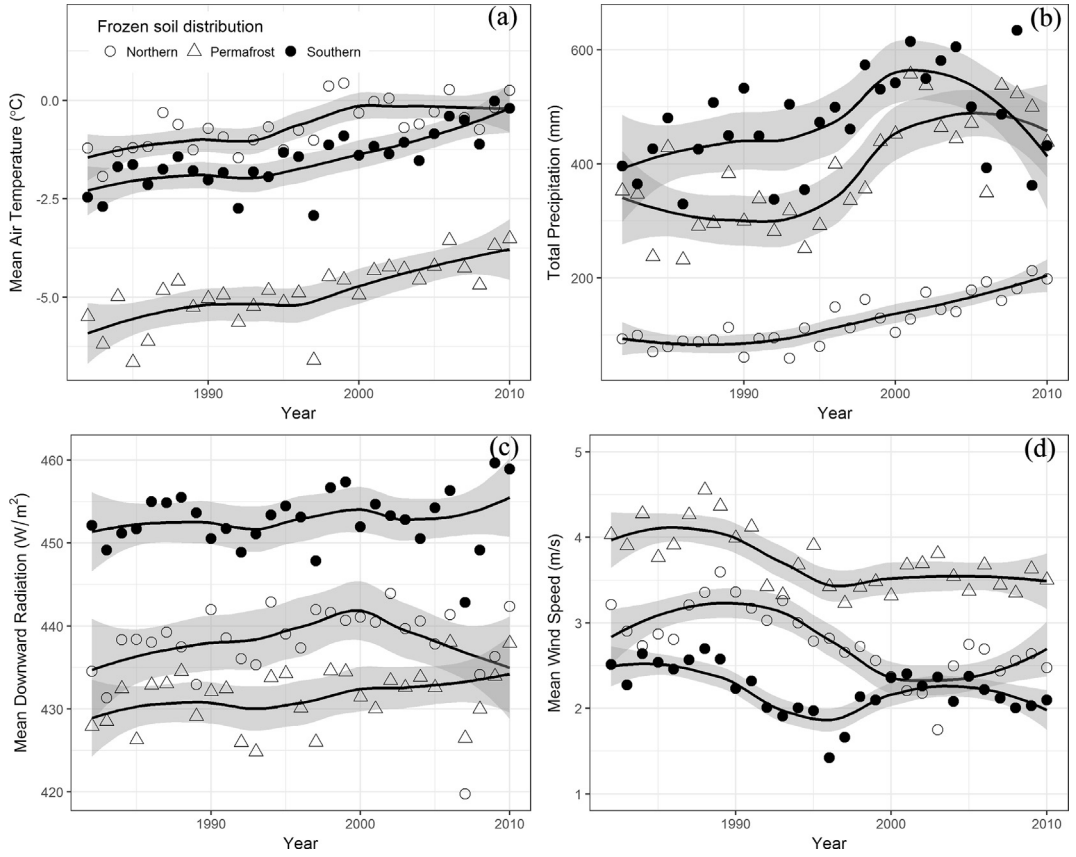

Fig. 2. Meteorological trends in three zones of the QTEC – northern, permafrost, and southern. (a) Annual mean air temperature (°C); (b) annual total precipitation (mm); (c) annual mean downward radiation (W/m^2); (d) annual mean wind speed (m/s).

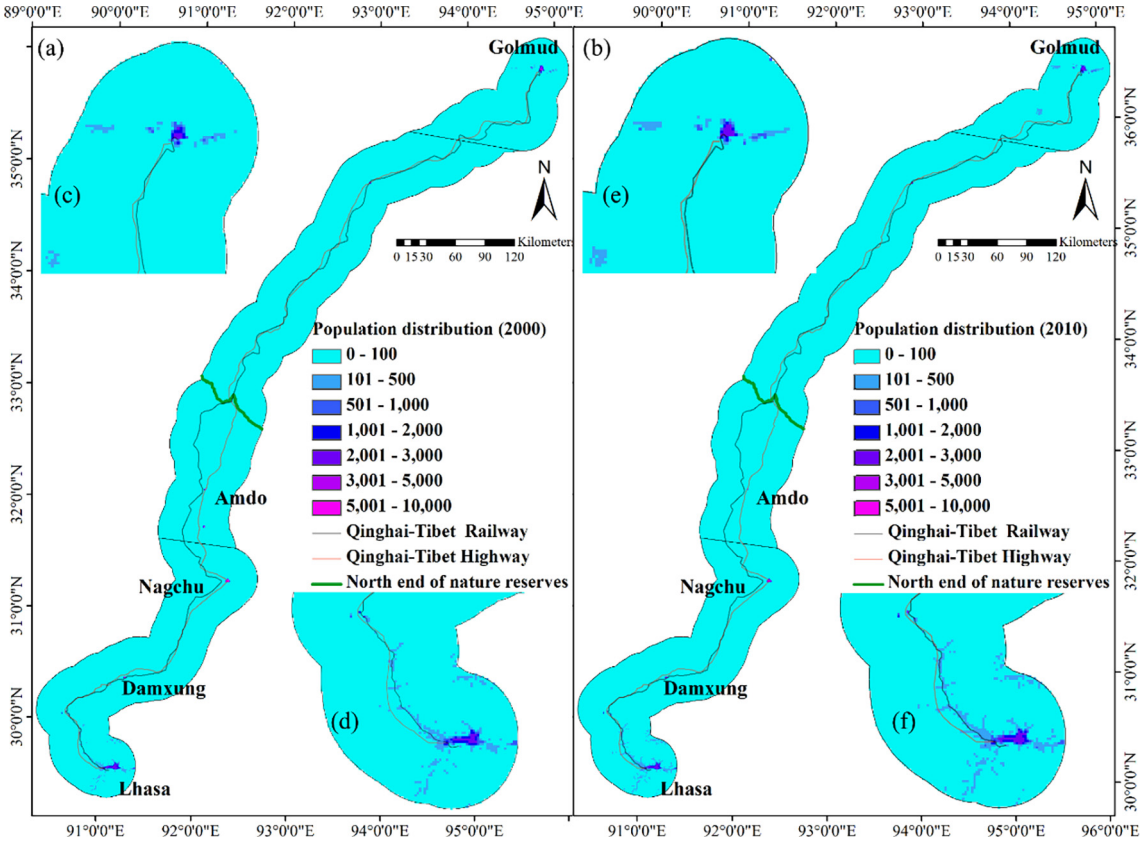

Fig. 3. Spatial distribution and density of permanent residents in the QTEC for 2000 and 2010. (a) Total population in 2000; (b) total population in 2010; (c) population in 2000 in the northern zone only; (d) population in 2000 in the southern zone only; (e) population in 2010 in the northern zone only; (f) population in 2010 in the southern zone only.

were less impacted by human activities than the other two zones.

Due to the unique natural environment and cultural characteristics, Tibet has long been a desirable travel destination for the people of China and abroad. However, tourism development in Tibet has been hindered by its remote and inaccessible location. Travel to Tibet has increased substantially since the opening of the QTR in 2006 (Su and Wall, 2009). As shown in Fig. 3, the spatial distribution of the population in the QTEC has a decentralized distribution pattern. The QTEC has 5 counties and county equivalents, and from north to south they are Golmud, Amdo, Nagqu, Damxung, and Lhasa, each with a city (Fig. 1). Amdo, Nagqu, Damxung, and Lhasa are in Tibet, while Golmud belongs to Qinghai. These five cities are also five stops on the QTR. There are additional smaller towns along the QTH, but the population is scarce throughout the area. Golmud is located in the northern zone, Amdo is located in the permafrost zone, and Nagqu, Damxung, and Lhasa are located in the southern zone. Golmud and Lhasa have much higher population densities than the other three cities. The trend of the spatial agglomeration of the population was more noticeable in 2010 than in 2000. The population density increased in all five cities from 2000 to 2010. At the same time, the population distribution and density along the QTR in the southern zone dispersed and increased with the construction and operation of the QTR. Since 2001, the number of permanent residents in Golmud and Lhasa experienced a significant increasing trend ($P < 0.05$). The population growth rates in the two periods (1982–2000, 2001–2010) were 38 and 42% in the northern zone, 15 and 27% in the permafrost, and 16 and 19% in the southern zone (Fig. 4a). The population growth rate of the latter period was higher than that of the previous period (Fig. 4a). The results showed that the intensity of human activity in the QTEC rose slowly before 2000 and rapidly after.

At the same time, the QTEC has become increasingly attractive as a transit point and a travel destination. In particular, the QTR has helped Qinghai and Tibet break through the transportation bottleneck that hindered the local economy (Li et al., 2016). It is especially important that Lhasa, which is a famous tourist destination in China, and the surrounding scenic spots have formed a transportation network centered in Lhasa. The tourist industry has grown rapidly, especially after the QTR opened to traffic in 2006. In 2007 alone, the number of tourists visiting the Potala Palace was more than 50 times that observed before the opening of the QTR (Qin and Zheng, 2010). The tourism boom and a massive influx of visitors boosted the economy immediately after the operation of the QTR began. The area surrounding Lhasa has become the most attractive in the QTP, with the number of tourists in that area far exceeding the number visiting other areas of the QTP. With the rapid growth of China's economy and infrastructure development in the QTEC, the numbers of visitors and permanent residents have increased. Interestingly, the number of tourists visiting Lhasa outnumber the resident population by more than 10 times (Fig. 4b).

There was a more than 75% increase in the goods carried to and from Lhasa by the QTR in 2010 (Li et al., 2016). Alpine meadows and shrubland used for grazing were the main vegetation types in the southern QTEC. The total number of livestock in the QTP showed a significant increase ($P < 0.001$) at a rate of $0.25 \times 10^6\,yr^{-1}$ in the study period, which was mainly due to an increase in the number of sheep (76% of the livestock). Amdo, Nagqu, and Damxung are traditional pastoral areas in Tibet. However, meat and milk outputs continue to increase in the three districts, even in Lhasa. The growth rates of meat and milk production in the southern QTEC after 2001 were much greater than the rates of the previous period (Fig. 4c).

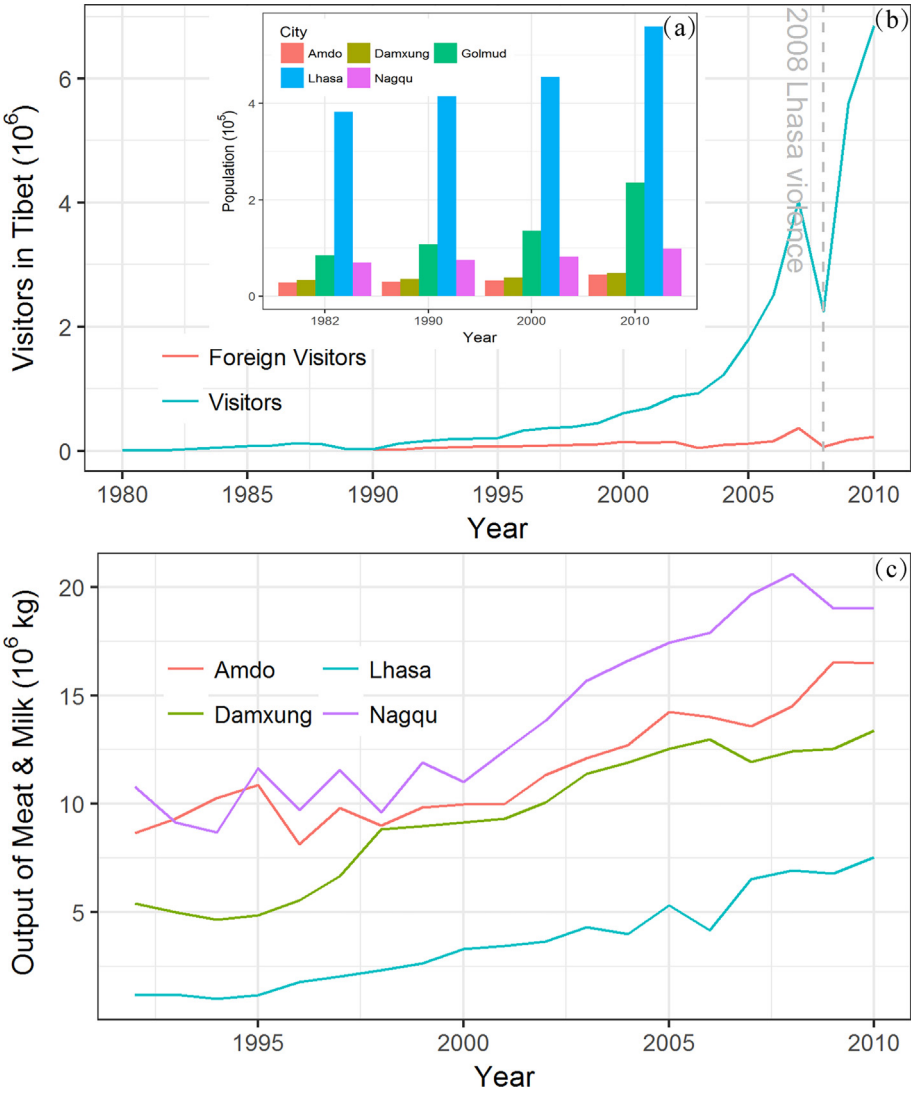

Fig. 4. Changes in population and meat and milk outputs. (a) Changes in permanent residents in the five largest cities in the QTEC from 1982 to 2010 (10^5); (b) number of visitors in Tibet from 1982 to 2010 (10^6); (c) meat and milk outputs in four cities in Tibet from 1992 to 2015 (10^6 kg).

3.3. Vegetation changes and their relationships to meteorological factors

The GIMMS NDVI data during the growing season exhibited a significant and positive increase at $0.0002\,yr^{-1}$ from 1982 to 2010 ($P < 0.001$). However, the GIMMS NDVI trends differed between the two periods, at $0.0010\,yr^{-1}$ for 1982–2000 and declined to $-0.0013\,yr^{-1}$ for 2001–2010 ($P < 0.001$); however, the trend in MODIS NDVI increased to $0.0021\,yr^{-1}$ for 2001–2010 ($P < 0.001$). In general, GIMMS NDVI declined in over 33% of the area over the past thirty years, and GIMMS and MODIS NDVI declined in over 50 and 22% of the area, respectively, over the past ten years (Fig. 5 and Table 2). Distinct differences in the growing season NDVI were detected among the zones, indicating zonality of vegetation. Overall, both declines and recoveries of greenness were detected in the three zones. During the period from 1982 to 2000, GIMMS NDVI increased significantly ($P < 0.001$) at rates of 0.0005, 0.0008, and $0.0018\,yr^{-1}$ from north to south, respectively. Vegetation declined in an average of 5% of the QTEC area, and accounted for 10, 4, and 1% of the northern, permafrost, and southern zones, respectively. In the period of 2001–2010, GIMMS NDVI increased at rate of 0.0014 and $0.0002\,yr^{-1}$ in the northern and permafrost zones, respectively; however, it declined at a rate of $-0.0046\,yr^{-1}$ in the southern zone, and these rates were significant for the northern and southern zones ($P < 0.001$); during the same period, MODIS NDVI increased at rates of 0.0043 and $0.0034\,yr^{-1}$ in the northern and permafrost zones, respectively, but declined at a rate of $-0.0055\,yr^{-1}$ in the southern zone, and these rates were significant all three zones ($P < 0.001$). On average, vegetation declined in 50 and 21% of the total area according to GIMMS and MODIS, respectively, and specifically, vegetation declined in 9 and 2, 39 and 5, and 84 and 53% of the northern, permafrost, and southern zones, respectively. According to the classification of vegetation, the results indicated that grasslands accounted for 77% of the vegetation deterioration in the southern zone, while shrublands, croplands and forestlands accounted for 9, 6 and 2%, respectively. The area of vegetation decline in the QTEC was greater from 2001 to 2010 than 1982 to 2000. The vegetation activity in the QTEC generally increased, especially in the northern zone; however, in the permafrost and southern zones, the area of vegetation degradation greatly increased. Furthermore, vegetation deterioration was more severe near the QTR and QTH in the southern part of the QTEC (Fig. 5).

The correlations between precipitation and GIMMS NDVI ($P < 0.05$) were significant and positive for the QTEC as a whole; this was observed for the entire and both the early and latter periods of the study (1982–2010, 1982–2000, and 2001–2010) (Table 3). In contrast, significantly negative correlations were found between air temperature and GIMMS NDVI during the early and latter periods ($P < 0.05$), and

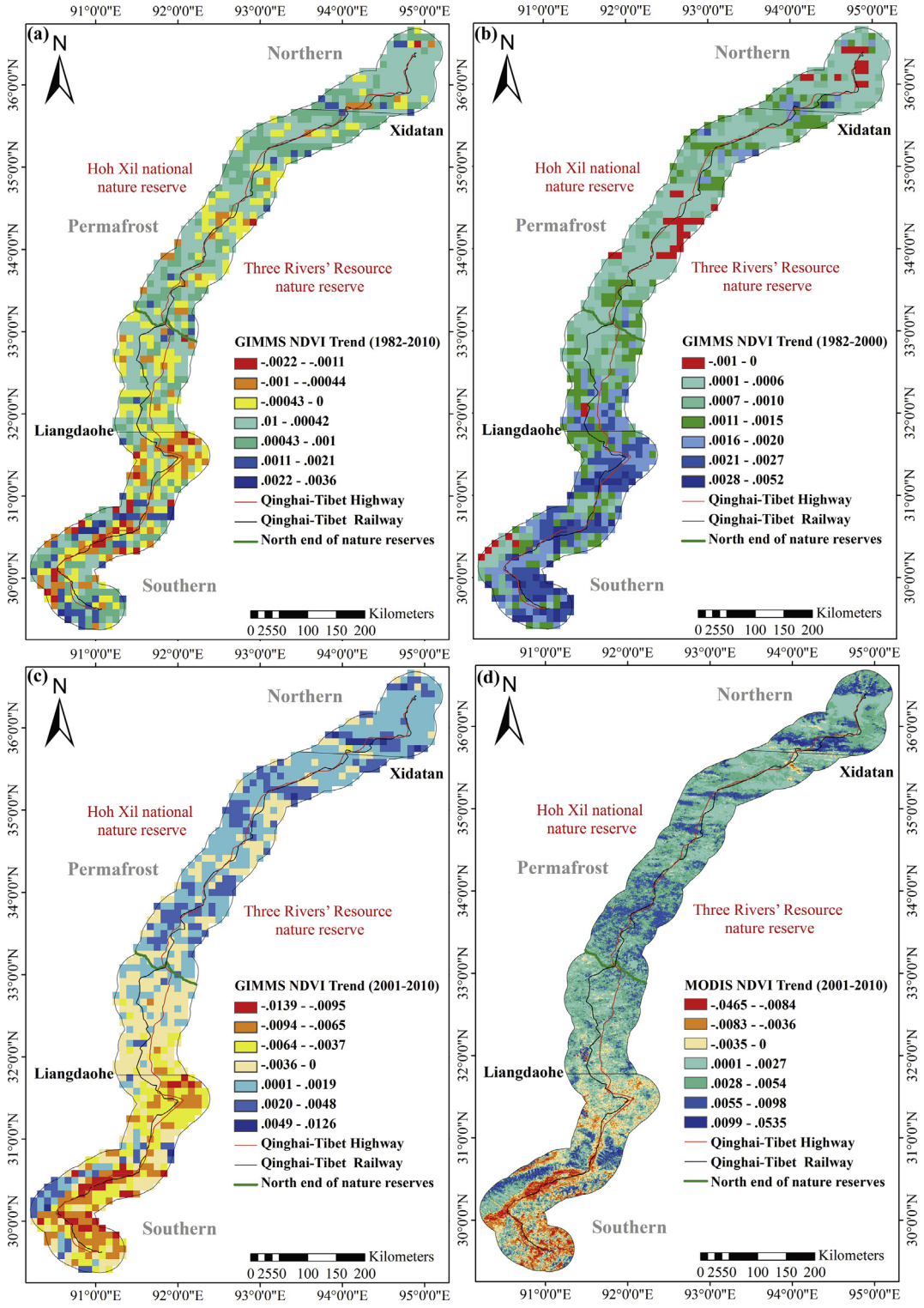

Fig. 5. Spatial distribution of growing-season NDVI for the different periods in the QTEC. (a) 1982–2010 for GIMMS; (b) 1982–2000 for GIMMS; (c) 2001–2010 for GIMMS; (d) 2001–2010 for MODIS. Changes are shown yr^{-1}.

at the same time, the downward radiation was strongly negatively correlated with GIMMS NDVI ($P < 0.05$). However, GIMMS NDVI exhibited a significantly positive correlation with wind speed from 2001 to 2010 ($P < 0.001$). During 2001–2010, the correlations between meteorological factors and MODIS NDVI presented similar characteristics. A significantly positive relationship between NDVI and precipitation suggested that precipitation was a favorable factor for the alpine ecosystem.

The spatial differences in meteorological factors across the QTEC affected the regional NDVI patterns. Thus, the vegetation and precipitation trends in the northern zone exhibited a significantly positive correlation for the period from 1982 to 2000 (Table 4). For the permafrost zone, precipitation and GIMMS NDVI exhibited significantly positive correlations for both 1982–2000 and 2001–2010 ($P < 0.001$), but the correlation coefficient for the latter was smaller than that for the previous period. In contrast, a strong negative correlation between

Table 2
Zonal trends in NDVI in the QTEC from 1982-2010. The values were significant at $P < 0.001$ (***), $P < 0.01$ (**), and $P < 0.05$ (*).

NDVI	1982–2010 (GIMMS)	1982–2000 (GIMMS)	2001–2010 (GIMMS)	2001–2010 (MODIS)
Northern	0.0003^{*}	0.0005^{*}	0.0014^{***}	0.0043^{***}
Permafrost	0.0002	0.0008^{**}	0.0002	0.0034^{***}
Southern	0.0001	0.0018^{**}	-0.0046^{***}	-0.0055^{***}

Table 3
Correlation coefficients between NDVI and meteorological factors in the QTEC. Values were significant at $P < 0.001$ (***), $P < 0.01$ (**), and $P < 0.05$ (*).

NDVI	Period	Precipitation	Air temperature	Wind speed	Downward radiation
GIMMS	1982–2010	0.07^{*}	−0.03	0.01	0.14^{*}
GIMMS	1982–2000	0.45^{***}	-0.23^{**}	0.02	-0.20^{**}
GIMMS	2001–2010	0.50^{***}	-0.56^{***}	0.36^{**}	-0.29^{**}
MODIS	2001–2010	0.57^{***}	-0.32^{*}	0.40^{*}	-0.21^{*}

air temperature and MODIS NDVI was found during 2001–2010 ($P < 0.001$), and at the same time, the downward solar radiation was strongly negatively correlated with the MODIS NDVI trends ($P < 0.05$). However, MODIS NDVI exhibited a significantly negative correlation with wind speed for the same period ($P < 0.01$). A significantly positive relationship between NDVI and precipitation trends suggested that precipitation was a favorable factor for the alpine ecosystem. We did not detect positive relationships in the southern zone. GIMMS NDVI and air temperature exhibited significantly negative correlations in the northern and permafrost zones for the two periods and a positive correlation in the southern zone. GIMMS NDVI had a stronger negative spatial correlation with wind speed in the northern and permafrost zones than in the southern zone in the early period. GIMMS NDVI and the downward radiation trends in the permafrost zone exhibited significantly negative correlations for the two periods. Because of the difference in resolution of the two NDVI datasets, the correlations between the two NDVI products and the meteorological factors are entirely different.

3.4. Active-layer variability and its relationships with meteorological factors

Permafrost areas began to shrink in the late 1960s from the southern end of the permafrost region near Liangdaohe to the northern end near Xidatan. Permafrost in the QTEC continued to thaw as the ALT increased (Fig. 6). The rate of ALT increase averaged 3 cm yr^{-1}. The rate from 2000 to 2010 was 4 cm yr^{-1}, which was greater than the rate of

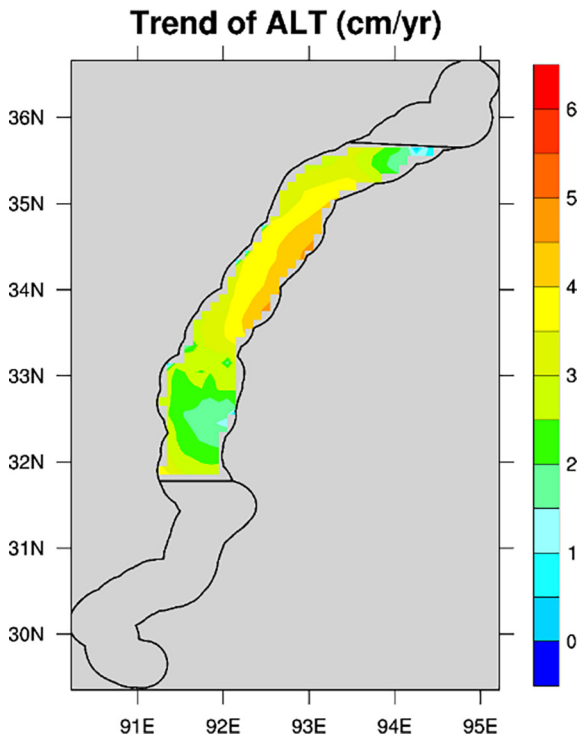

Fig. 6. The spatial trend of ALT from 1982 to 2010.

2 cm yr^{-1} from 1982 to 2000. In recent decades, the rate of permafrost thawing increased significantly, and the central region of the permafrost zone exhibited the greatest change, which is consistent with the air temperature trends in that region. The relationships between ALT and air temperature, and ALT and downward radiation exhibited significantly positive correlations, indicating that the significantly positive trend of active layer thickening was a response to increased air temperature and downward radiation ($P < 0.01$) throughout the period from 1982 to 2010 (Table 5).

The linear slope of the regression of the observations against the simulation over 10 sites was 0.21, and the coefficient reached 0.77 (Fig. 7). A comparison of the results showed that the simulated ALT data matched the observed data ($P < 0.01$), although the simulated rate of ALT increase was generally less than the observed increase. The simulated results showed that the ALT has increased over the last 30 years, and the ALT was between 0.83 and 2.42 m with a mean value of 1.75 m. The comparison of the simulation results and the observed values along the QTH indicated that the observed ALT was greater than that obtained in the simulation.

Table 4
Correlation coefficients for NDVI and meteorological factors in the three zones of the QTEC. Values were significant at $P < 0.001$ (***), $P < 0.01$ (**), and $P < 0.05$ (*).

NDVI	Period	Zones	Precipitation	Air temperature	Wind speed	Downward radiation
GIMMS	1982–2010	Northern	−0.07	0.11	-0.24^{**}	0.01
		Permafrost	0.04	−0.04	-0.20^{**}	0.02
		Southern	0.09	0.02	0.05	0.03
GIMMS	1982–2000	Northern	0.45^{***}	-0.12^{*}	-0.29^{***}	0.08
		Permafrost	0.50^{***}	-0.32^{**}	-0.26^{**}	-0.35^{***}
		Southern	−0.10	0.32^{**}	0.12	−0.05
GIMMS	2001–2010	Northern	−0.08	-0.15^{*}	0.08	−0.12
		Permafrost	0.37^{***}	-0.26^{**}	0.05	-0.46^{***}
		Southern	−0.04	-0.11^{*}	0.03	−0.09
MODIS	2001–2010	Northern	0.39^{**}	−0.09	0.21^{*}	0.01
		Permafrost	0.07	0.23^{**}	-0.10^{*}	0.01
		Southern	−0.05	0.08	−0.02	0.00

Table 5
Correlation coefficients between ALT and meteorological factors in the permafrost zone of the QTEC. Values were significant at $P < 0.001$ (***), $P < 0.01$ (**), and $P < 0.05$ (*).

ALT	Precipitation	Air temperature	Wind speed	Downward radiation
1982–2010	0.08	0.24***	0.06	0.14**

3.5. Effects of alpine vegetation on permafrost

Because the spatial resolution of MODIS NDVI is far beyond the resolution of the simulated ALT data, and GIMMS NDVI and ALT have the same study period, so GIMMS NDVI was selected in this study. All negative NDVI values in the two periods and the corresponding ALT values were selected to analyze the relationship between vegetation deterioration and permafrost degradation. As shown in Fig. 8, the spatial pattern of the negative NDVI values was significantly and negatively correlated with ALT for the two periods ($R = -0.58$, $P < 0.001$), which indicated that permafrost degradation has potential negative effects on alpine vegetation activity, or, if occurring simultaneously, vegetation loss can induce a retreat and eventual disappearance of permafrost.

The negative NDVI values were transformed to positive values and used to analyze the potential effects of vegetation improvement on permafrost to assess whether alpine vegetation can shield the perennially frozen ground from incoming radiation. As shown in Fig. 9, there was a significantly negative correlation between vegetation and downward radiation in the permafrost zone for the two periods ($R = -0.17$, $P < 0.001$), indicating that improvement in vegetation conditions could reduce the effect of incoming radiation. The positive NDVI trends were not significantly negatively correlated with the ALT for the QTEC in the two periods of study ($R = 0.06$ and $P > 0.05$ for 1982–2000, $R = 0.10$ and $P > 0.05$ for 2001–2010). These results suggested that increasing vegetation activity may not exert a significantly negative effect on permafrost thawing.

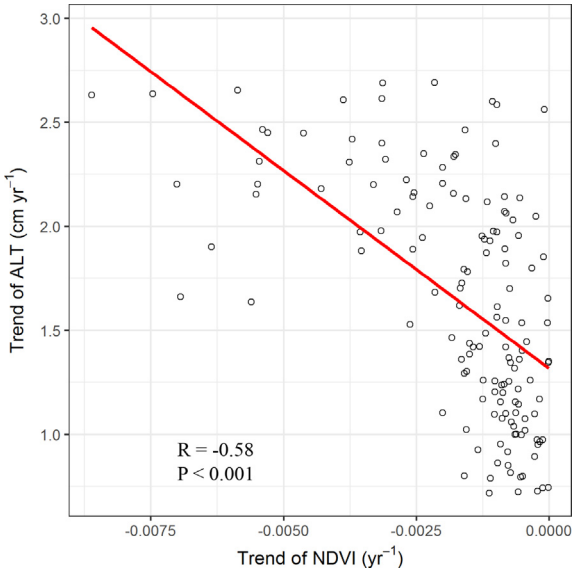

Fig. 8. Spatial relationships of negative GIMMS NDVI and ALT. The *red line* denotes the corresponding trend. (For interpretation of the references to colour in this figure legend, the reader is referred to the web version of this article.)

4. Discussion

4.1. Changes in alpine vegetation in response to climate change and human activities

Climate change and human activities are major drivers of changes in terrestrial ecosystems (Chen et al., 2014; Field, 2001), but it is very difficult to directly distinguish their impacts on these ecosystems (Chen et al., 2014). The QTEC experienced a significant warming and wetting trend, with direct and rapid effects on the alpine ecosystem. The corridor and the QTP presented similar climate change trends, but the increase in air temperature of the corridor was greater than that in the QTP (Jin et al., 2008). The total annual precipitation decreased from south to north; this confirmed the spatial patterns of precipitation that are generally recognized to exhibit a decreasing trend from southeast to northwest and from south to north and then gradually weaken. The results showed that the NDVI over the alpine areas of the QTEC increased over the past thirty years, but the rates of increase differed for the three zones and the two periods of study (1982–2000 and 2001–2010). The total annual precipitation in the northern zone was much less than that in the permafrost or southern zones. Spatially, the changes in NDVI were most strongly correlated with precipitation. Strong correlations indicated that the positive vegetation greenness trend was a response to increased precipitation (Cuo et al., 2016). The negative correlations between NDVI and air temperature indicated that increasing air temperature adversely affected the growth of alpine vegetation in the latter period (Zhang et al., 2013). The regional vegetation change in the QTP was also found to be related to increased precipitation (Piao et al., 2004).

Human activities can also profoundly affect vegetation. Socio-

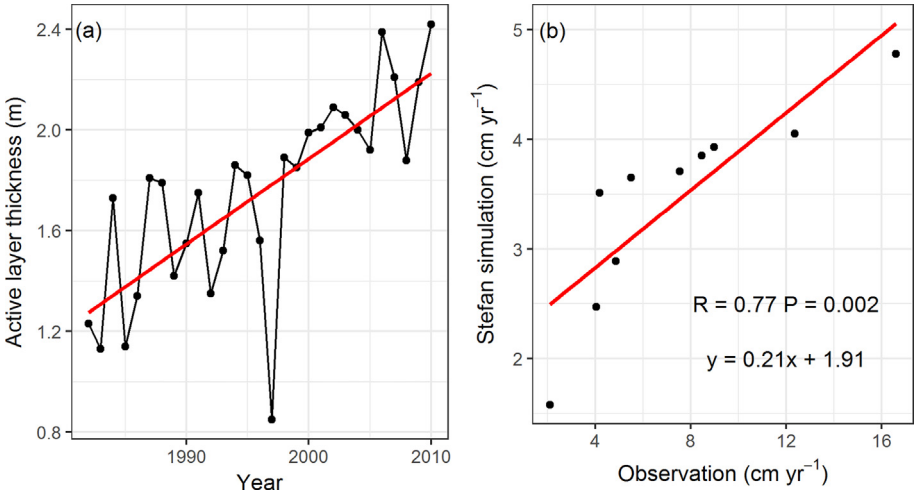

Fig. 7. Active layer thickness (ALT). (a) Simulated maximum thawing depth in the permafrost zone; (b) the relationship between the observed and simulated rate of ALT increase for 10 monitoring sites along the Qinghai-Tibetan Highway. The *red line* denotes the corresponding trend. (For interpretation of the references to colour in this figure legend, the reader is referred to the web version of this article.)

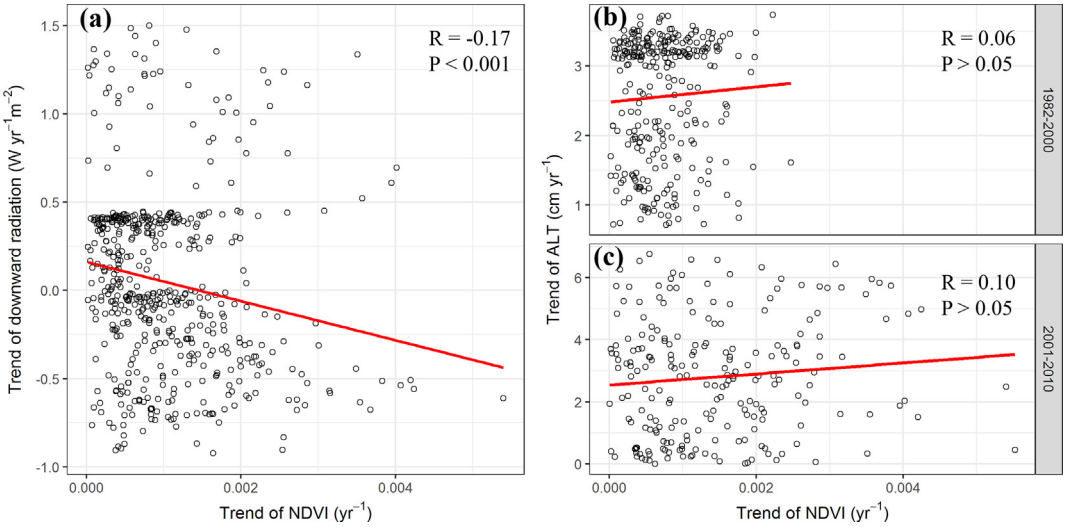

Fig. 9. Spatial relationships between the positive GIMMS NDVI values, downward radiation and ALT. (a) Trends of positive GIMMS NDVI and downward radiation. (b) Trends of positive GIMMS NDVI and ALT for 1982–2000; (c) trends of positive GIMMS NDVI and ALT for 2001–2010. The *red line* denotes the corresponding trend. (For interpretation of the references to colour in this figure legend, the reader is referred to the web version of this article.)

economic drivers began to exceed the forces of nature over the QTP in 2000. Economic development generated a strong demand for livestock, including sheep, yak, horse, donkey, mule, and camel, and led to rapid development of livestock-raising, human population growth, increased transport of goods, and growing exploitation of natural resources (Qin and Zheng, 2010). Grasslands exhibited the most severe degradation of the vegetation types in the southern QTEC from Amdo to Lhasa, which is the main source of grazing. These results suggest that grazing may be one of the major causes of grassland degradation. The increase in passenger traffic resulted in greater tourism and economic activity. The sharply increasing population and rapid increases in grazing resulted in the regional degradation of the alpine vegetation (Harris, 2010; Yu et al., 2012). The increased utilization of resources that allowed the growth in tourism led to further vegetation degradation in the southern zone and the southern parts of the permafrost zone. The environmental impacts of the QTR and QTH are an ongoing concern. Since 2001, the vegetation in the area surrounding Lhasa, including the two nature reserves in the southern zone near Lhasa, has experienced varying degrees of degradation. Furthermore, vegetation in the southern zone is even worse, especially along the QTR and QTH. These results suggested that the construction and operation of the QTR sped up tourism developments since 2001 and brought about the deterioration of the surrounding alpine vegetation (Li et al., 2016; Qin and Zheng, 2010).

To slow down the environmental degradation in the QTP, China established large-scale conservation programs, including Grain-for-Green in 1999 and Grazing Withdrawal in 2003. These programs included fencing of degraded grasslands, ecological compensation, and restoration of land cover (Chen et al., 2014, 2013). The increase of the NDVI in the permafrost zone may be due to a series of national policies in China that were established for the protection and restoration of grasslands. With two nature reserves in the permafrost zone, the vegetation achieved a certain degree of recovery during the two periods of study. Amdo is located in the permafrost zone next to nature reserves, but both population and grazing activity have significantly increased in the area since 2001. The establishment of nature reserves was designed to reduce the encroachment of human activities to a certain extent. The trends in human activities in Amdo and the nature reserves in the permafrost zone since 2001 were vastly opposite, and the area of decreased NDVI is much larger than the area of nature reserves in 2001. The effects of annual meat and milk production on the annual average NDVI in Tibet were evaluated for the periods of 1992–2000 and 2001–2010. Meat and milk production in the earlier phase was negatively correlated with NDVI ($R = -0.05$), and there was a significantly negative correlation between them ($R = -0.54$, $P < 0.05$). This result indicated that human activities played an important role in the vegetation changes. The correlation between precipitation and NDVI in the three zones weakened in the latter period, but it was still significantly positive for the permafrost zone. This result indicated that, with the intensification of human activities, the increase in precipitation in the early period enhanced vegetation activity, and the increase in human activities in the latter period reduced vegetation activity. Overall, the impacts of human activities on alpine vegetation in the latter period were greater than the impacts of increased precipitation in the earlier period.

4.2. Permafrost dynamics in response to climate change and human activities

Variations in air temperature were the driving forces in the permafrost temperature dynamics. Permafrost has been retreating and degrading at a rapid rate due to the combined influence of steadily increasing human activities and persistent climatic warming. In recent decades, increasing surface air temperatures have played a key role in triggering permafrost degradation (Riseborough et al., 2008). Moreover, permafrost in the QTEC has degraded at both ends, with the degradation in the southern reaches being more striking than that in the northern area. Long-term temperature measurements indicated that the lower altitudinal limit of permafrost has moved up by 25 m over the last 30 years in the north, and it has moved between 50 and 80 m over the last 20 years in the south (Cheng and Wu, 2007). Permafrost in both the southern and the northern zones thawed, and both zones were more affected by human activities than the permafrost zone. The significantly positive correlation between air temperature, downward radiation, and ALT suggested that increasing air temperature and incoming radiation accelerated the thawing of permafrost. However, increasing ALT was mainly influenced by the rise in air temperature ($P < 0.001$). Such an increase in air temperature can warm the ground through energy exchange at the surface, which results in significant permafrost degradation. Extensive and accelerated degradation of permafrost has also been observed in response to climate warming along the QTEC (Jin et al., 2008). The rate of observed ALT increase ranged from 1.33 to 16.60 cm yr^{-1} (Wu and Zhang, 2010), while the simulated rate was from 0.87 to 4.92 cm yr^{-1}. In another study in the same region, the rate of simulated average ALT increase was less than the 7.5 cm yr^{-1} of the

observed average ALT increase (Wu and Zhang (2010). The average ALT observed along the QTH was 2.41 m, and the range was 1.32–4.57 m (Wu and Zhang, 2010). The reasons for the differences were that the observation sites near the QTH were influenced by human activities (Li et al., 2012), and the observation period was within the simulated period and fell within the latter part, which was characterized by rapid permafrost thawing.

The Stefan solution and most of the permafrost models did not consider the effects of human activities. Moreover, the majority of the observational sites for the active layer and permafrost temperatures in the QTEC were located in the vicinity of the QTR and QTH to facilitate access to measurement sites. Previous studies also showed that the ALT values near the QTR and QTH were greater than those in other regions (Li et al., 2012). This result showed that the intensification of human activities also played an important role in the degradation of permafrost.

4.3. Spatial relationships between alpine vegetation and permafrost

Vegetation exerts significant effects on hydrothermal processes and the spatial distribution of permafrost (Guglielmin et al., 2014). Vegetation also controls the incoming radiation, snow accumulation, soil organic content, and capacity for water storage, all of which greatly influence the thermal and moisture regimes of permafrost (Runyan and D'Odorico, 2012). Increased vegetation activity may be a cooling factor for the underlying soils (Kaufmann et al., 2003), offsetting permafrost warming despite an increase in air temperature. For the QTEC, it currently unknown whether changes in alpine vegetation contributed to permafrost variability. Deterioration of vegetation occurred in association with permafrost degradation (Yang et al., 2013; Yi et al., 2014). A recent study indicated that vegetation deterioration accompanied an increase in the ALT in the alpine ecosystems in the QTP (Chen et al., 2014). In our study, an overall improvement in the condition of alpine vegetation cannot necessarily prevent the degradation of permafrost, and vegetation improvement was insufficient to reverse the permafrost degradation caused by warming. Large uncertainties are associated with the soil thermal parametrizations of the Stefan solution. However, the majority of the permafrost zones in our study were alpine steppe, which may be one of the reasons why vegetation could not inhibit the degradation of permafrost, although the improvement of vegetation was significantly negatively correlated with incoming radiation. Nevertheless, it is still unclear how the restoration of alpine vegetation would affect the permafrost. Hence, it is necessary to analyze the effects of different alpine vegetation on permafrost and determine their relationships with field monitoring and experiments.

At the same time, degradation of permafrost has the potential to significantly affect soil moisture content and soil nutrient availability, thereby affecting vegetation growth (Bowden et al., 2008). Accompanying permafrost degradation, soil moisture and soil organic matter also declined in the QTP permafrost regions (Wang et al., 2014; Yang et al., 2013; Yi et al., 2011). In the region of seasonally frozen soil adjacent to the permafrost in the QTEC, the vegetation exhibited more serious deterioration. A decrease in alpine vegetation activity often occurred in the region adjacent to permafrost and seasonally frozen soil, indicating that the change from permanently to seasonally frozen soil can degrade vegetation, or, perhaps occurring simultaneously, vegetation loss can induce a retreat of and eventual disappearance of permafrost. These results implied that permafrost degradation was disadvantageous to the stability of alpine vegetation. This study focuses on the influence of alpine vegetation on permafrost from a spatial perspective and could not fully consider the interactions between alpine vegetation and permafrost. Therefore, these interactions represent one potential area for future research on this subject.

4.4. Data and model uncertainties

Because of the difficulty of access during parts of the study, some measurements of atmospheric, ground, and human activity variables were not available. In addition, remote sensing-based products are affected by uncertainties resulting from physical limitations of the sensor, limited spatiotemporal coverage, and spatial resolution (Knoche et al., 2014). The ALT was simulated with the gridded climatic data sets to estimate the frozen soil status and possible changes over the QTEC. There were also differences in ALT between adjacent observation sites because the permafrost was affected by local environmental variables, such as vegetation, snow cover, slope, and aspect. Moreover, each grid represented a specified portion of the study area, which resulted in large uncertainties in the comparisons between the grid simulations and field observations. Indeed, changes in ALT need further validation. At present, gridded ALT simulations do not consider the uncertainties and changes in surface and subsurface conditions caused by climate warming and disturbances, such as vegetation changes, snow cover, land use changes, soil moisture changes, fire disturbance, and freeze–thaw hazards, in the input parameters (Riseborough et al., 2008). Moreover, different spatial scales of ALT simulations can translate into uncertainty (Anisimov et al., 2007). This condition may underestimate the changes in ALT because high human activity and vegetation degeneration can accelerate degradation of permafrost from the warming of the atmospheric climate. Data uncertainties and Stefan solution limitations prevented us from reaching a quantitative conclusion on the permafrost dynamics that were induced by increased vegetation activity. Data were analyzed from the perspective of spatial correlation only, and future field experiments are needed to explore the effects of alpine vegetation improvement on permafrost and the effect of permafrost degradation on alpine vegetation. These limitations can be significant for ALT dynamics under changing environmental conditions.

5. Conclusions

Climate change and human activities significantly impact the alpine ecosystem throughout the QTEC. Our data confirmed increases in the mean annual air temperature, total precipitation, and downward radiation and a decreasing trend in surface wind speed over the QTEC. Increased total precipitation improved the vegetation conditions across much of the QTEC, while increased air temperatures accelerated the thaw of permafrost, as it became warmer and wetter in recent decades. The vegetation has degraded in some areas, especially in the southern QTEC. Moreover, vegetation deterioration was more severe in the southern zone near the QTR and QTH. The deterioration of the alpine vegetation in the area was due to increases in the numbers of visitors and permanent residents and greater economic activity since the construction and operation of the QTR. Grazing, transportation, engineering disturbance, and changes in land cover have modified and sometimes amplified these impacts. Although the trend of increasing air temperature and precipitation suggested a warming and wetting phenomenon over the QTEC, increased human activity could render the ecosystems more vulnerable to permafrost degradation. The deterioration of vegetation was influenced by human activities, and the degradation of permafrost was affected by air temperature. Our results demonstrated the great potential for understanding complex interactions between vegetation and permafrost under climate change and human activities based on remote sensing products and permafrost simulations.

Acknowledgements

Data were obtained from NASA GES DISC (https://disc.gsfc.nasa.gov), NASA Earth Exchange (https://nex.nasa.gov/nex), WestDC (https://westdc.westgis.ac.cn), GsCloud (https://www.gscloud.cn), China meteorological data network (https://data.cma.cn), and Global

Change Research Data Publishing and Repository (http://www.geodoi.ac.cn). This research was supported by the National Natural Science Foundation of China (41301508, 41630636). We would like to express our gratitude to the editors and reviewers for suggestions for improvement of this paper.

Appendix A. Supplementary data

Supplementary data associated with this article can be found, in the online version, at http://dx.doi.org/10.1016/j.ecolind.2018.04.067. These data include Google maps of the most important areas described in this article.

References

Anisimov, O.A., Lobanov, V.A., Reneva, S.A., Shiklomanov, N.I., Zhang, T.J., Nelson, F.E., 2007. Uncertainties in gridded air temperature fields and effects on predictive active layer modeling. J. Geophys. Res. Earth 112.

Bontemps, S., Defourny, P., Bogaert, E.V., Arino, O., Kalogirou, V., Perez, J.R., 2011. GLOBCOVER 2009-Products Description and Validation Report.

Bothe, O., Fraedrich, K., Zhu, X.H., 2011. Large-scale circulations and Tibetan Plateau summer drought and wetness in a high-resolution climate model. Int. J. Climatol. 31, 832–846.

Bowden, W.B., Gooseff, M.N., Balser, A., Green, A., Peterson, B.J., Bradford, J., 2008. Sediment and nutrient delivery from thermokarst features in the foothills of the North Slope, Alaska: potential impacts on headwater stream ecosystems. J. Geophys. Res. 113.

Chen, B.X., Zhang, X.Z., Tao, J., Wu, J.S., Wang, J.S., Shi, P.L., Zhang, Y.J., Yu, C.Q., 2014. The impact of climate change and anthropogenic activities on alpine grassland over the Qinghai-Tibet Plateau. Agric. For. Meteorol. 189, 11–18.

Chen, H., Zhu, Q.A., Peng, C.H., Wu, N., Wang, Y.F., Fang, X.Q., Gao, Y.H., Zhu, D., Yang, G., Tian, J.Q., Kang, X.M., Piao, S.L., Ouyang, H., Xiang, W.H., Luo, Z.B., Jiang, H., Song, X.Z., Zhang, Y., Yu, G.R., Zhao, X.Q., Gong, P., Yao, T.D., Wu, J.H., 2013. The impacts of climate change and human activities on biogeochemical cycles on the Qinghai-Tibetan Plateau. Global Change Biol. 19, 2940–2955.

Chen, P.Y., Fedosejevs, G., Tiscareno-Lopez, M., Arnold, J.G., 2006. Assessment of MODIS-EVI, MODIS-NDVI and VEGETATION-NDVI composite data using agricultural measurements: an example at corn fields in western Mexico. Environ. Monit. Assess. 119, 69–82.

Cheng, G.D., Wu, T.H., 2007. Responses of permafrost to climate change and their environmental significance, Qinghai-Tibet Plateau. J. Geophys. Res. 112.

Coughlan, M., Avissar, R., 1996. The global energy and water cycle experiment (GEWEX) continental-scale international project (GCIP): an overview. J. Geophys. Res. 101, 7139–7147.

Cuo, L., Zhang, Y.X., Piao, S.L., Gao, Y.H., 2016. Simulated annual changes in plant functional types and their responses to climate change on the northern Tibetan Plateau. Biogeosciences 13, 3533–3548.

Fan, J., Yong, X.U., Wang, C.S., Niu, Y.F., Chen, D., Sun, W., 2015. The effects of human activities on the ecological environment of Tibet over the past half century (in Chinese). Chin. Sci. Bull. 60, 3057.

Field, C.B., 2001. Global change - Sharing the garden. Science 294, 2490–2491.

Fu, J.Y., Jiang, D., Huang, Y.H., 2014. 1 KM Grid Population Dataset of China (PopulationGrid_China), V1 ed. Global Change Research Data Publishing & Repository.

Guglielmin, M., Fratte, M., Cannone, N., 2014. Permafrost warming and vegetation changes in continental Antarctica. Environ. Res. Lett. 9.

Harris, R.B., 2010. Rangeland degradation on the Qinghai-Tibetan plateau: a review of the evidence of its magnitude and causes. J. Arid Environ. 74, 1–12.

Hilbich, C., Hauck, C., Hoelzle, M., Scherler, M., Schudel, L., Voelksch, I., Muehll, D.V., Maeusbacher, R., 2008. Monitoring mountain permafrost evolution using electrical resistivity tomography: a 7-year study of seasonal, annual, and long-term variations at Schilthorn, Swiss Alps. J. Geophys. Res. 113.

Huffman, G.J., Bolvin, D.T., Nelkin, E.J., Wolff, D.B., Adler, R.F., Gu, G., Hong, Y., Bowman, K.P., Stocker, E.F., 2007. The TRMM multisatellite precipitation analysis (TMPA): quasi-global, multiyear, combined-sensor precipitation estimates at fine scales. J. Hydrometeorol. 8, 38–55.

Jin, H.J., Yu, Q.H., Wang, S.L., Lu, L.Z., 2008. Changes in permafrost environments along the Qinghai-Tibet engineering corridor induced by anthropogenic activities and climate warming. Cold Regions Sci. Technol. 53, 317–333.

Kaufmann, R.K., Zhou, L., Myneni, R.B., Tucker, C.J., Slayback, D., Shabanov, N.V., Pinzon, J., 2003. The effect of vegetation on surface temperature: a statistical analysis of NDVI and climate data. Geophys. Res. Lett. 30.

Knoche, M., Fischer, C., Pohl, E., Krause, P., Merz, R., 2014. Combined uncertainty of hydrological model complexity and satellite-based forcing data evaluated in two data-scarce semi-arid catchments in Ethiopia. J. Hydrol. 519, 2049–2066.

Li, L., Yang, S., Wang, Z.Y., Zhu, X.D., Tang, H.Y., 2010. Evidence of warming and wetting climate over the Qinghai-Tibet Plateau. Arctic Antarctic Alpine Res. 42, 449–457.

Li, R., Zhao, L., Ding, Y.J., Wu, T.H., Xiao, Y., Du, E.J., Liu, G.Y., Qiao, Y.P., 2012. Temporal and spatial variations of the active layer along the Qinghai-Tibet Highway in a permafrost region. Chin. Sci. Bull. 57, 4609–4616.

Li, S., Wang, Z., Zhang, Y., Wang, Y., Liu, F., 2016. Comparison of socioeconomic factors between surrounding and non-surrounding areas of the Qinghai-Tibet railway before and after its construction. Sustainability Basel 8, 776.

Liu, Y.M., Wu, G.X., Hong, J.L., Dong, B.W., Duan, A.M., Bao, Q., Zhou, L.J., 2012. Revisiting Asian monsoon formation and change associated with Tibetan Plateau forcing: II. Change. Clim. Dynam. 39, 1183–1195.

Luo, L., Ma, W., Zhang, Z., Zhuang, Y., Zhang, Y., Yang, J., Cao, X., Liang, S., Mu, Y., 2017. Freeze/thaw-induced deformation monitoring and assessment of the slope in permafrost based on terrestrial laser scanner and GNSS. Remote Sens. Basel 9, 198.

Nachtergaele, F., Velthuizen, H.V., Verelst, L., Batjes, N., Dijkshoorn, K., Engelen, V.V., Fischer, G., Jones, A., Montanarella, L., Petri, M., 2009. Harmonized world soil database, world congress of soil science: soil solutions for a changing world, Brisbane, Australia, 1–6 August 2010. In: Symposium 1.2.1 Global Soil Spatial Information Systems, pp. 34–37 (Published on DVD).

Nelson, F.E., Shiklomanov, N.I., Mueller, G.R., Hinkel, K.M., Walker, D.A., Bockheim, J.G., 1997. Estimating active-layer thickness over a large region: Kuparuk River Basin, Alaska, USA. Arctic Antarctic Alpine Res. 29, 367–378.

Nemani, R., Hashimoto, H., Votava, P., Melton, F., Wang, W., Michaelis, A., Mutch, L., Milesi, C., Hiatt, S., White, M., 2009. Monitoring and forecasting ecosystem dynamics using the terrestrial observation and prediction system (TOPS). Remote Sens. Environ. 113, 1497–1509.

Piao, S.L., Fang, J.Y., Ji, W., Guo, Q.H., Ke, J.H., Tao, S., 2004. Variation in a satellite-based vegetation index in relation to climate in China. J. Veg. Sci. 15, 219–226.

Qin, Y., Zheng, B., 2010. The Qinghai-Tibet railway: a landmark project and its subsequent environmental challenges. Environ. Dev. Sustain. 12, 859–873.

Riseborough, D., Shiklomanov, N., Etzelmuller, B., Gruber, S., Marchenko, S., 2008. Recent advances in permafrost modelling. Permafrost Periglacial Process. 19, 137–156.

Royleveillee, P., Burn, C., Mcdonald, I., 2014. Vegetation-permafrost relations within the forest-tundra ecotone near Old Crow, Northern Yukon, Canada. Permafrost Periglacial Process. 25, 127–135.

Rui, H., Beaudoing, H., 2011. Readme Document for Global Land Data Assimilation System Version 2 (GLDAS-2) Products. GES DISC.

Runyan, C.W., D'Odorico, P., 2012. Ecohydrological feedbacks between permafrost and vegetation dynamics. Adv. Water Resour. 49, 1–12.

Sazonova, T., Romanovsky, V., 2003. A model for regional-scale estimation of temporal and spatial variability of active layer thickness and mean annual ground temperatures. Permafrost Periglacial Process. 14, 125–139.

Shen, M.G., Piao, S.L., Jeong, S.J., Zhou, L.M., Zeng, Z.Z., Ciais, P., Chen, D.L., Huang, M.T., Jin, C.S., Li, L.Z.X., Li, Y., Myneni, R.B., Yang, K., Zhang, G.X., Zhang, Y.J., Yao, T.D., 2015. Evaporative cooling over the Tibetan Plateau induced by vegetation growth. Proc. Natl. Acad. Sci. U.S.A. 112, 9299–9304.

Su, M.M., Wall, G., 2009. The Qinghai-Tibet railway and Tibetan tourism: Travelers' perspectives. Tourism Manage. 30, 650–657.

Wang, G.X., Mao, T.X., Chang, J., Du, J.Z., 2014. Impacts of surface soil organic content on the soil thermal dynamics of alpine meadows in permafrost regions: data from field observations. Geoderma 232, 414–425.

White, D.C., Lewis, M.M., Green, G., Gotch, T.B., 2016. A generalizable NDVI-based wetland delineation indicator for remote monitoring of groundwater flows in the Australian Great Artesian Basin. Ecol. Indic. 60, 1309–1320.

Wu, G.X., Duan, A.M., Liu, Y.M., Mao, J.Y., Ren, R.C., Bao, Q., He, B., Liu, B.Q., Hu, W.T., 2015a. Tibetan Plateau climate dynamics: recent research progress and outlook. Natl. Sci. Rev. 2, 100–116.

Wu, Q.B., Hou, Y.D., Yun, H.B., Liu, Y.Z., 2015b. Changes in active-layer thickness and near-surface permafrost between 2002 and 2012 in alpine ecosystems, Qinghai-Xizang (Tibet) Plateau, China. Global Planet Change 124, 149–155.

Wu, Q.B., Zhang, T.J., 2010. Changes in active layer thickness over the Qinghai-Tibetan Plateau from 1995 to 2007. J. Geophys. Res. 115.

Yang, Z.P., Gao, J.X., Zhao, L., Xu, X.L., Ouyang, H., 2013. Linking thaw depth with soil moisture and plant community composition: effects of permafrost degradation on alpine ecosystems on the Qinghai-Tibet Plateau. Plant Soil 367, 687–700.

Yi, S.H., Wang, X.Y., Qin, Y., Xiang, B., Ding, Y.J., 2014. Responses of alpine grassland on Qinghai-Tibetan plateau to climate warming and permafrost degradation: a modeling perspective. Environ. Res. Lett. 9.

Yi, S.H., Zhou, Z.Y., Ren, S.L., Xu, M., Qin, Y., Chen, S.Y., Ye, B.S., 2011. Effects of permafrost degradation on alpine grassland in a semi-arid basin on the Qinghai-Tibetan Plateau. Environ. Res. Lett. 6.

Yu, C.Q., Zhang, Y.J., Claus, H., Zeng, R., Zhang, X.Z., Wang, J.S., 2012. Ecological and environmental issues faced by a developing tibet. Environ. Sci. Technol. 46, 1979–1980.

Zhang, L., Guo, H., Ji, L., Lei, L., Wang, C., Yan, D., Li, B., Li, J., 2013. Vegetation greenness trend (2000–2009) and the climate controls in the Qinghai-Tibetan Plateau. J. Appl. Remote Sens. 7.